Intermetallics 33 (2013) 16–26

Contents lists available at SciVerse ScienceDirect

Intermetallics

journal homepage: www.elsevier.com/locate/intermet

# On the U–Cu–Al and U–Cu–Ga systems at 600 °C

Yu. Verbovytskyy*, A.P. Gonçalves

*IST/ITN, Instituto Superior Técnico, Universidade Técnica de Lisboa and CFMC-UL, Estrada Nacional 10, P-2686-953 Sacavém Codex, Portugal*

ARTICLE INFO

*Article history:*
Received 13 August 2012
Received in revised form
6 September 2012
Accepted 7 September 2012
Available online 11 November 2012

*Keywords:*
A. Ternary alloy systems
B. Phase diagrams
B. Phase identification
F. Diffraction
F. Electron microscopy
F. Scanning

ABSTRACT

The phase relations in the U–Cu–Al and U–Cu–Ga systems have been studied at 600 °C in concentration region of 0–45/75 at.% Al and 0–40/75 at.% Ga, respectively. X-ray diffraction techniques, optical microscopy and scanning electronic microscopy, complemented with energy dispersive X-ray spectroscopy (EDS), were used to identify the phases and characterize their crystal structures and compositions. Five new ternary phases have been identified for the first time: $UCu_{6+x}Al_{5-x}$ ($x \sim 0$–$0.2$) ($TbCu_{6.4}Al_{4.6}$ structure type), $UCu_{6+x}Al_{5-x}$ ($x \sim 0.38$–$0.68$) ($BaCd_{11}$ structure type), $U_{2-\varepsilon}(Cu_{7+x}Ga_{10-x})_{1+\delta}$ ($\varepsilon \sim 0.5$, $\delta \sim 0.03$, $x \sim 0.5$–$1$) (related to $Th_2Ni_{17}$ structure type), $UCu_{5+x}Ga_{1-x}$ ($x \sim 0$–$0.7$) ($CeCu_6$ structure type) and $U_{14}Cu_{44+x}Ga_{7-x}$ ($x \sim 0.5$–$2.5$) (related to $Gd_{14}Ag_{51}$ structure type). The crystal structure of the $UCu_{5+x}Ga_{1-x}$ and $U_{14}Cu_{44+x}Ga_{7-x}$ intermetallics has been determined from X-ray single crystal counter data.

## 1. Introduction

The production of new materials with pre-defined physical and chemical properties is one of the most important aims of modern technology. Uranium based compounds and alloys occupy an important place among them. Moreover, due to the unusual behaviour of many uranium based intermetallic phases, they are also interesting from the scientific point of view. Those compounds exhibit a great variety of physical phenomena, such as long range exotic magnetic order, spin-glass behaviour, Kondo effects, heavy fermion ground state, unconventional superconductivity, intermediate valence state etc. It is considered that these electronic features are mainly related to the degree of hybridization between the 5*f* and *s*, *p* and *d* orbitals of neighbour atoms. The best way for finding and studying the conditions of the formation of ternary compounds is the systematic oriented investigation of the phase diagrams, which reflects the phase composition of the alloys and gives information on the conditions of the compounds formation (stability of the compounds, transformation of the structures versus composition and temperature).

Many uranium-based alloy systems and intermetallic compounds have been already studied. However, a big lack of data on some uranium – *d*– and *p*–metals interactions still occur among them. For example, summarized data on interaction among the components in the U – *d*–metal – {Al, Ga, In} systems are displayed in the Table 1. Up to our best knowledge, the systematic oriented investigations were mainly performed on the systems with 4*d* metals, and only some specific compositions were studied in the other ones. In total, twelve isothermal sections were constructed and the existence of 132 ternary phases has been described in the literature [1–5] and references herein. We have stopped our attention on the U–Cu–Al and U–Cu–Ga systems. Herein, we present isothermal sections of above mentioned systems at 600 °C and crystal structure determination of the new ternary phases.

## 2. Literature data

### 2.1. Binary systems

A brief summary of the literature data focussing on phase equilibrium of the binary U–Cu–(Al, Ga) subsystems is presented here.

The U–Al system was studied by Gordon and Kaufmann [6]. Three binary compounds exist in this system: $UAl_4$ (own type), $UAl_3$ ($AuCu_3$-type) and $UAl_2$ ($MgCu_2$-type). The U–Ga phase diagram was constructed by Buschow [7]; at least three binary compounds have been identified in above mentioned system: $UGa_3$ ($AuCu_3$-type), $UGa_2$ ($AlB_2$-type) and $U_3Ga_5$ ($Pu_3Pd_5$-type). Interaction between the components in the U–Cu system [8] is characterized by the formation of only one compound, $UCu_5$, with $AuBu_5$ structure type.

---

* Corresponding author.
*E-mail address:* yuryvv@bigmir.net (Yu. Verbovytskyy).

0966-9795/$ – see front matter © 2012 Elsevier Ltd. All rights reserved.
http://dx.doi.org/10.1016/j.intermet.2012.09.024

**Table 1**
Summarized data on the ternary U–M–{Al, Ga, In} systems.

| Ti | V | Cr | Mn | Fe | Co | Ni | Cu | Zn |
|---|---|---|---|---|---|---|---|---|
| ☐ (1) | ☐ (2) | ☐ (3) | ■ (2)<br>☐ (1) | ■ (7)<br>■ (7) | ■ (7)<br>■ (10)<br>■ (2) | ■ (5)<br>■ (8)<br>■ (4) | ☐ (7)<br>☐ (4)<br>■ (2) | |
| Zr | Nb | Mo | Tc | Ru | Rh | Pd | Ag | Cd |
| ■ (0) | ☐ (2) | ■ (3) | | ☐ (3)<br>☐ (3)<br>☐ (1) | ☐ (2)<br>☐ (5)<br>☐ (3) | ☐ (2)<br>☐ (5)<br>☐ (3) | | |
| Hf | Ta | W | Re | Os | Ir | Pt | Au | Hg |
| | ☐ (2) | ☐ (2) | | ☐ (1)<br>☐ (1) | ☐ (3)<br>☐ (3)<br>☐ (2) | ☐ (1)<br>☐ (3)<br>☐ (3) | ☐ (3)<br>☐ (2)<br>☐ (1) | |

Cu – M.
☐ (7) – R–M–Al system.
☐ (4) – R–M–Ga system.
■ (2) – R–M–In system.
Phase equilibrium is established in the whole concentration region or in a part of it (■), only separate alloys have been investigated (☐). Lack of a symbol means the system has not yet been investigated. (N) – Number of ternary compounds.

Interaction between the components in the Cu–Al [9,10] and Cu–Ga [11,12] system has a complex character. Fourteen ($CuAl_2$, rt– and ht–CuAl, rt– and ht–$Cu_4Al_3$, ht1– and ht2–$Cu_3Al_2$, $Cu_{33}Al_{17}$, rt– and ht–$Cu_9Al_4$, $Cu_7Al_3$, rt– and ht–$Cu_3Al$, $Cu_4Al$) and eight ($CuGa_2$, $Cu_3Ga_2$, $Cu_2Ga$, rt– and ht–$Cu_9Ga_4$, rt–, ht1– and ht2–$Cu_4Ga$) intermediate phases have been established, respectively. More detailed information on the composition and structure of these phases can be found in supplementary data (Table S1–S2).

### 2.2. Ternary systems

There is no data in the literature on the investigation of the phase diagram of the U–Cu–Al and U–Cu–Ga systems. However, the crystal structure and properties of certain ternary U–Cu–{Al, Ga} compounds were widely studied [13–19] and references herein. Due to the large number of publications we referred only papers where certain phases were reported for first time. Seven ternary phases are known from the U–Cu–Al system: $UCuAl_2$ ($TiAl_3$-type) [14], $U_3Cu_2Al$ ($MgZn_2$-type) [14], $U_2Cu_9Al$ ($MgZn_2$-type) [15], $UCu_{3+x}Al_{2-x}$ ($x \sim 0$–$0.5$) ($CaCu_5$-type) [15,16], $UCu_5Al$ ($YbMo_2Al_4$-type) [17], $U_2Cu_{7+x}Al_{10-x}$ ($Th_2Zn_{17}$-type) ($x \sim 0$–$5$) [18,19] and $UCu_{4+x}Al_{8-x}$ ($x \sim 0$–$2$) ($ThMn_{12}$-type) [18,20]. The existence of five ternary gallides have been described up to now: $U_2Cu_{7+x}Ga_{10-x}$ ($x \sim 0.7$–$5$) ($Th_2Zn_{17}$-type) [19,21], $UCu_{1+x}Ga_{3-x}$ ($x \sim 0.33$–$0.5$) ($BaAl_4$-type) [22], $UCu_{3+x}Ga_{2-x}$ ($x \sim 0$–$0.8$) ($CaCu_5$-type) [23,24], UCuGa ($CaIn_2$-type or LiGaGe-type) [25,26], $UCu_xGa_{2-x}$ ($x \sim 0$–$0.56$) ($Lu_2CoGa_3$-type at $x = 0.5$ and $AlB_2$-type at $x \neq 0.5$) [26,27].

## 3. Experimental details

Metals with nominal purities 99.95 wt.% (uranium ingots), 99.99 wt.% (copper rod and plate), 99.95 wt.% (aluminium spheres) and 99.995 wt.% (gallium pieces) were used as a starting materials. A total of 64 (U–Cu–Al system) and 78 (U–Cu–Ga system) binary and ternary samples with a total weight 0.5–1.0 g were prepared by arc-melting the elements under argon atmosphere. The products were re-melted at least three times in order to ensure homogeneity. Finally, alloys were defragmented into small pieces, sealed in evacuated quartz tubes under vacuum ($10^{-5}$ Torr) and annealed at 600 °C for one month. After the heat treatments, the samples were quenched, by submerging the quartz tubes in cold water, and analysed.

The polycrystalline products were crushed, powdered with agate mortar and examined by X-ray diffraction. X-ray phase and structural analysis were performed using a PANalitical X'Pert Pro diffractometer (Cu K$\alpha$-radiation). The scans were taken in the $\theta/2\theta$ mode with the following parameters: $2\theta$ region 15–120°; step scan 0.03°; counting time per step 2–20 s. The theoretical powder patterns were calculated with the help of the PowderCell program [28]. The lattice parameters were obtained by least-squares fitting using the Latcon program [29]. The FullProf [30] program was used for Rietveld refinements. Pseudo-Voigt profile shape function was used. The background was refined with a polynomial function. Results of these fittings of selected phases are given in supplementary data (Table S3).

Single crystals suitable for X-ray diffraction measurements were selected from the crushed samples obtained by slowly cooling from 1000 °C to room temperature within 10 h. The single crystal intensity data were collected at room temperature using a four-circle Enraf–Nonius Mach III diffractometer with graphite monochromatized Mo K$\alpha$-radiation and a scintillation counter with pulse height discrimination. Scans were taken in the $\omega/2\theta$ mode. Empirical absorption corrections were applied on the basis of $\Psi$-scan data. The crystal structures were refined using Shelxl-97 [31] (full-matrix least-squares on $F^2$). The unit cell parameters were obtained by least-squares refinement of the $2\theta$ values of 25 intense and well-centred reflections from various parts of the reciprocal space ($15° < 2\theta < 35°$).

The microstructure of the samples was first studied on polished and etched surfaces, by using an optical microscope Olympus OM150. Selected samples were then observed by electron microscopy, by using a JEOL JSM-T330A scanning electron microscope (SEM) operated at 25 kV. The composition phases were also analysed by semi-quantitative energy dispersive X-ray spectroscopy (EDS). At least three valid EDS point analyses were made for each phase in order to guarantee a good analysis of their compositions. These analyses were carried out with a spatial resolution of ~2 μm and a collection time of 200 s. The AnalySIS 3.0 (from Soft Imaging System GmbH) and Quest SpectraPlus (from Termo Noran) softwares were used.

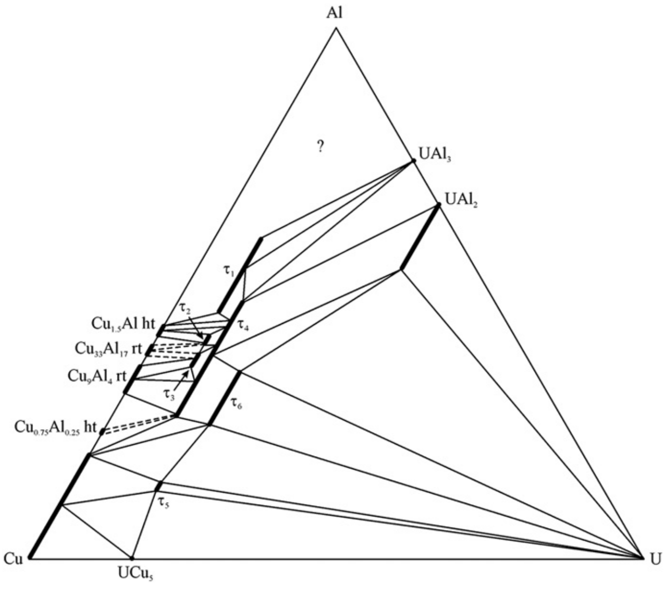

**Fig. 1.** Isothermal section of the U–Cu–Al system at 600 °C. Ternary phases: ($\tau_1$) $UCu_{4+x}Al_{8-x}$ ($0 \le x \le 2$); ($\tau_2$) $UCu_{6+x}Al_{5-x}$ ($0 \le x \le 0.2$); ($\tau_3$) $UCu_{6+x}Al_{5-x}$ ($0.38 \le x \le 0.68$); ($\tau_4$) $U_2Cu_{7+x}Al_{10-x}$ ($0.6 \le x \le 5$); ($\tau_5$) $UCu_{5+x}Al_{1-x}$ ($0 \le x \le 0.18$); ($\tau_6$) $UCu_{3+x}Al_{2-x}$ ($0 \le x \le 0.5$).

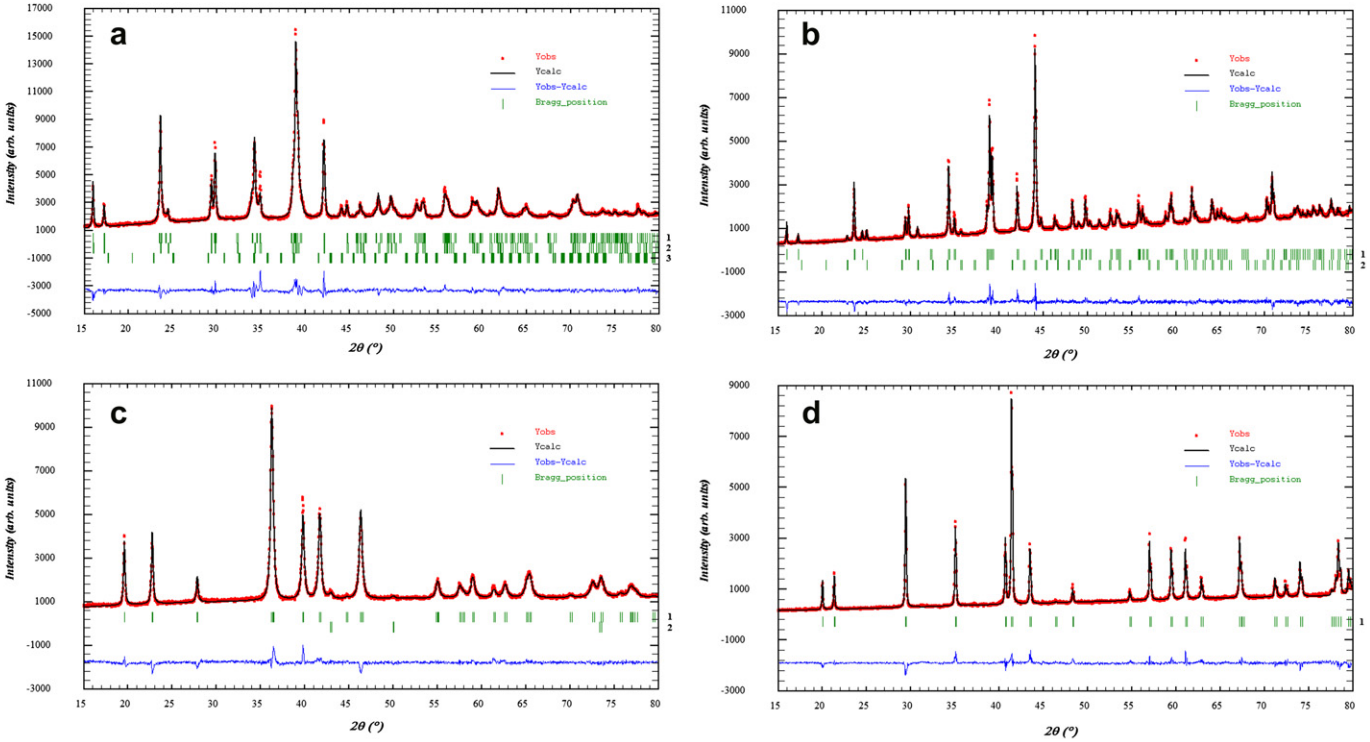

**Fig. 2.** X-ray diffraction patterns of selected U–Cu–Al alloys: (a) $U_8Cu_{52}Al_{40}$ (1 – $\tau_2$, 2 – $\tau_3$, 3 – $Cu_{33}Al_{17}$ rt); (b) $U_5Cu_{61}Al_{34}$ (1 – $\tau_3$, 2 – $Cu_9Al_4$ rt); (c) $U_{14}Cu_{74}Al_{12}$ (1 – $\tau_5$, 2 – Cu); (d) $U_{17}Cu_{55}Al_{28}$ (1 – $\tau_6$).

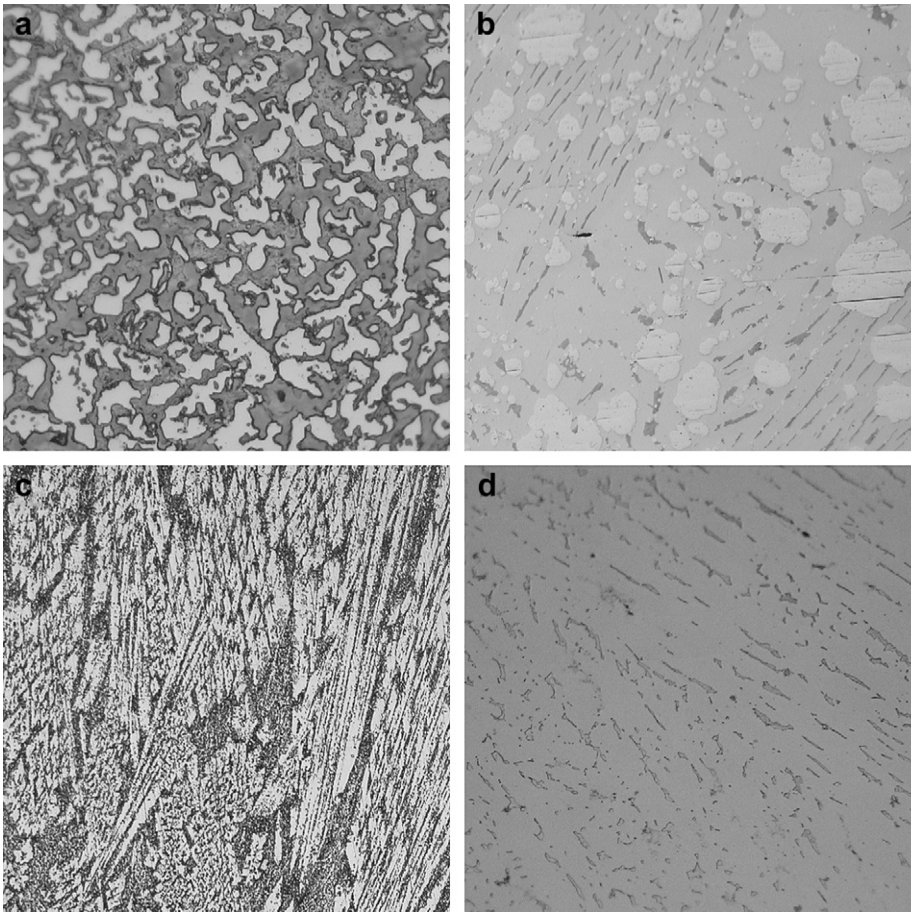

**Fig. 3.** Microphotographs of selected U–Cu–Al alloys: (a) $U_{25}Cu_{25}Al_{50}$ (×500), (b) $U_{33}Cu_{50}Al_{17}$ (×200), (c) $U_{17}Cu_{75}A_{l8}$ (×100) and (d) $U_8Cu_{52}Al_{40}$ (×200).

**Table 2**
Ternary phases from the U–Cu–Al system.

| Phase | Structure type | Space group | Lattice parameters | | | | $x$ |
|---|---|---|---|---|---|---|---|
| | | | $a$ | $b$ | $c$ | $V$ | |
| $UCu_{4+x}Al_{8-x}$ ($\tau_1$) | $ThMn_{12}$ | $I4/mmm$ | 8.7938(2) | – | 5.1232(1) | 396.18(2) | 0 |
| | | | 8.7402(2) | – | 5.1038(1) | 389.89(2) | 1 |
| | | | 8.7096(4) | – | 5.0664(2) | 384.33(3) | 2 |
| $UCu_{6+x}Al_{5-x}$ ($\tau_2$) | $TbCu_{6.4}Al_{4.6}$ | $Fddd$ | 14.2730(7) | 14.9077(9) | 6.5818(3) | 1400.46(13) | 0 |
| | | | 14.4102(11) | 14.6926(10) | 6.5843(5) | 1394.05(18) | 0.2 |
| $UCu_{6+x}Al_{5-x}$ ($\tau_3$) | $BaCd_{11}$ | $I4_1/amd$ | 10.2822(5) | – | 6.5802(4) | 695.69(6) | 0.38 |
| | | | 10.2471(4) | – | 6.5883(3) | 691.78(4) | 0.68 |
| $U_2Cu_{7+x}Al_{10-x}$ ($\tau_4$) | $Th_2Zn_{17}$ | $R\overline{3}m$ | 8.8227(5) | – | 12.8817(8) | 868.38(9) | 0.6 |
| | | | 8.8118(2) | – | 12.8706(4) | 865.49(4) | 1 |
| | | | 8.7866(2) | – | 12.8263(4) | 857.58(4) | 2 |
| | | | 8.7426(3) | – | 12.7712(6) | 845.36(6) | 3 |
| | | | 8.7195(4) | – | 12.7542(7) | 839.78(7) | 4 |
| | | | 8.7055(5) | – | 12.6926(8) | 833.05(9) | 5 |
| $UCu_{5+x}Al_{1-x}$ ($\tau_5$) | $YbMo_2Al_4$ | $I4/mmm$ | 6.4136(4) | – | 4.9506(4) | 203.64(2) | 0 |
| | | | 6.4044(3) | – | 4.9294(3) | 202.19(2) | 0.18 |
| $UCu_{3+x}Al_{2-x}$ ($\tau_6$) | $CaCu_5$ | $P6/mmm$ | 5.1363(4) | – | 4.1614(3) | 95.07(1) | 0 |
| | | | 5.1070(1) | – | 4.1619(1) | 94.01(1) | 0.3 |
| | | | 5.0979(2) | – | 4.1605(2) | 93.64(1) | 0.5 |

## 4. Results and discussion

### 4.1. The U–Cu–Al system

The isothermal section at 600 °C of the U–Cu–Al phase diagram in concentration region of 0–45/75 at.% Al is presented in Fig. 1. X-ray diffraction patterns and microstructures of selected U–Cu–Al annealed alloys are illustrated in Figs. 2 and 3, respectively.

The uranium-based binary $UAl_3$ ($AuCu_3$-type), $UAl_2$ ($MgCu_2$-type) and $UCu_5$ ($AuBe_5$-type) compounds were usually detected in the Al- or Cu-rich region of the U–Cu–Al system. Moreover, the binary $UAl_2$ compound was found to dissolve ~12 at.% Cu. According to the Cu–Al phase diagram, the $Cu_{1-x}Al_x$ (Cu-rich solid solution) (Cu-type), ht–$Cu_{0.75}Al_{0.25}$ (W-type), rt–$Cu_9Al_4$ (own-type), rt–$Cu_{33}Al_{17}$ (own-type), ht–$Cu_{1.5}Al$ ($Ni_2In$-type) and ht–CuAl (own-type) phases are stable at 600 °C. Some of them were observed in annealed ternary alloys from the Cu-rich region. Questionable equilibrium lines from this region are presented by broken lines.

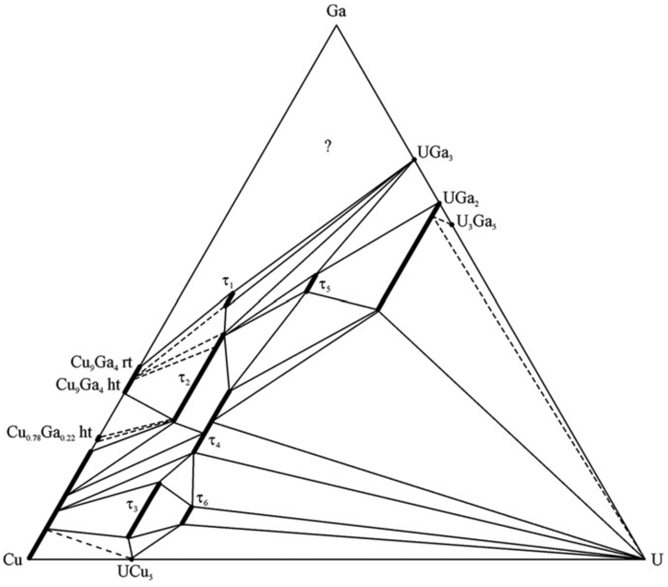

**Fig. 4.** Isothermal section of the U–Cu–Ga system at 600 °C. Ternary phases: ($\tau_1$) $U_{2-\varepsilon}(Cu_{7+x}Ga_{10-x})_{1+\delta}$ ($\varepsilon \sim 0.5$, $\delta \sim 0.03$, $0.5 \leq x \leq 1$); ($\tau_2$) $U_2Cu_{7+x}Ga_{10-x}$ ($2 \leq x \leq 5$); ($\tau_3$) $UCu_{5+x}Ga_{1-x}$ ($0 \leq x \leq 0.7$); ($\tau_4$) $UCu_{3+x}Ga_{2-x}$ ($0 \leq x \leq 0.8$); ($\tau_5$) $UCu_{1+x}Ga_{3-x}$ ($0.35 \leq x \leq 0.5$); ($\tau_6$) $U_{14}Cu_{44+x}Ga_{7-x}$ ($0.5 \leq x \leq 2.5$).

The existence of the four early reported ternary $UCu_{4+x}Al_{8-x}$ ($x \sim 0$–2) ($ThMn_{12}$-type) ($\tau_1$), $U_2Cu_{7+x}Al_{10-x}$ ($x \sim 0.6$–5) ($Th_2Zn_{17}$-type) ($\tau_4$), $UCu_5Al$ ($YbMo_2Al_4$-type) ($\tau_5$) and $UCu_{3+x}Al_{2-x}$ ($x \sim 0$–0.5) ($CaCu_5$-type) ($\tau_6$) phases has been confirmed by the present work and their homogeneity ranges were verified on a basis of X-ray diffraction data. Calculated lattice parameters of above mentioned phases are given in Table 2. It should be also noted that the $UCu_5Al$ compound was observed to have a small homogeneity range, dissolving ~2 at.% Cu(Al), and that the previous reported co-existence of two phases with the same $CaCu_5$-type in the annealed at 600 °C $UCu_{3+x}Al_{2-x}$ alloys with $x \sim 0.3$ [32] was not detected.

Formation of the early reported $UCuAl_2$ ($TiAl_3$-type) $U_2Cu_3Al$ ($MgZn_2$-type) and $U_2Cu_9Al$ ($MgZn_2$-type) intermetallic compounds were not confirmed at 600 °C. It is supposed that these ternaries can exist at other temperatures or stabilize by impurities. Corresponded annealed samples were not single phase and contained other phases ($U_{25}Cu_{25}Al_{50}$ ($\tau_4$, $\tau_6$, and solid solution based on $UAl_2$); $U_{33}Cu_{50}Al_{17}$ ($\tau_5$, $\tau_6$, and α-U); $U_{17}Cu_{75}Al_8$ ($\tau_5$ and $UCu_5$) (Fig. 3a–c).

In the annealed alloys with composition along the cross-section with 8.3 at.% uranium two new ternary $UCu_{6+x}Al_{5-x}$ phases with $x \sim 0$–0.2 ($\tau_2$) and $x \sim 0.38$–0.68 ($\tau_3$) were found. On the basis of primary analysis of the X-ray diffraction data the orthorhombic $TbCu_{6.4}Al_{4.6}$ and tetragonal $BaCd_{11}$ structure types were assigned for the above sited phases. Lattice parameters are presented in Table 2. Synthesis of the single phase samples, accurate crystal structure determination, magnetic and transport properties of these phases will be published in a further paper.

### 4.2. The U–Cu–Ga system

Based on X-ray phase and microstructure analysis the isothermal section of the U–Cu–Ga system at 600 °C was constructed in the 0–40/75 at.% Ga concentration range and is presented in Fig. 4. X-ray diffraction patterns and microstructures of some U–Cu–Ga annealed alloys are shown in Figs. 5 and 6, respectively.

The formation of the binary $UGa_3$ ($AuCu_3$-type), $UGa_2$ ($AlB_2$-type), $U_3Ga_5$ ($Pu_3Pd_5$-type) and $UCu_5$ ($AuBe_5$-type) compounds were confirmed to exist at 600 °C. The previously reported solubility of copper in $UGa_2$ was also confirmed: $UGa_2$ dissolves up to

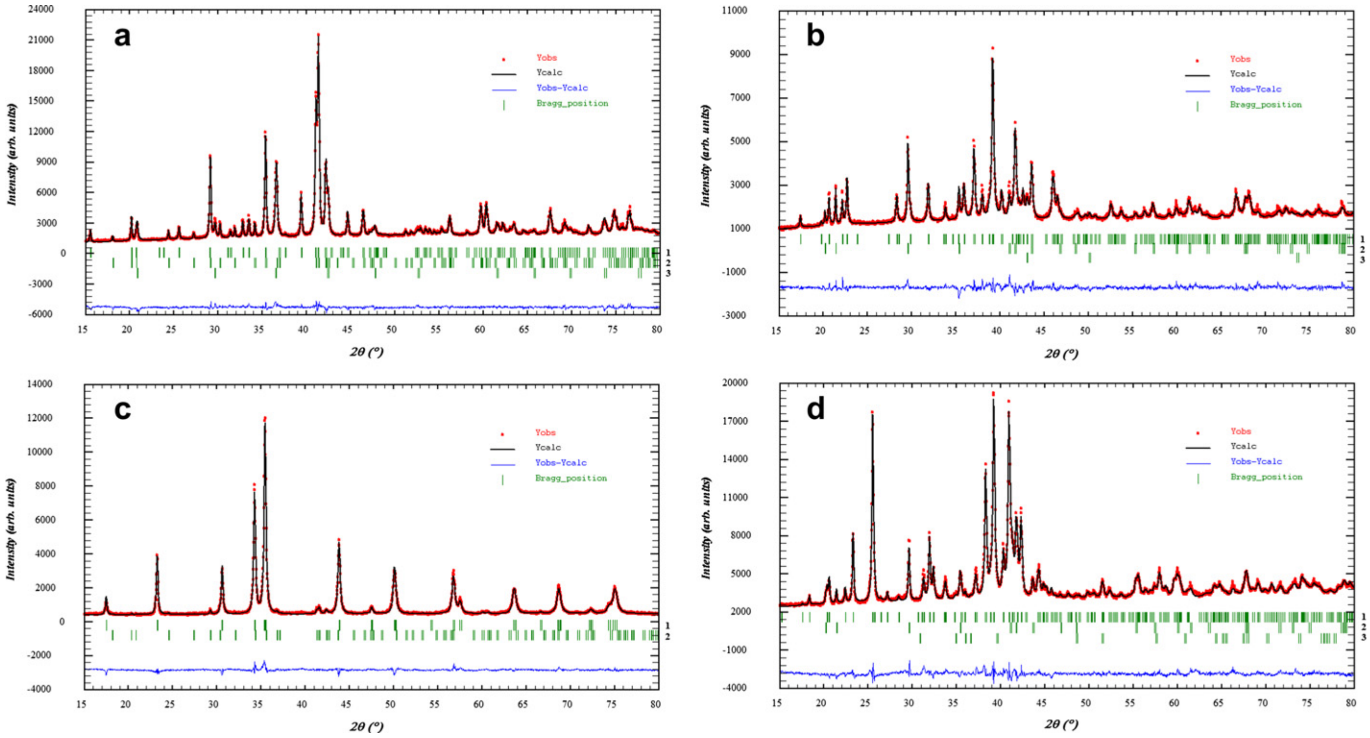

**Fig. 5.** X-ray diffraction patterns of selected U–Cu–Ga alloys: (a) $U_{10}Cu_{42}Ga_{48}$ (1 – $\tau_1$, 2 – $\tau_2$, 3 – $UGa_3$); (b) $U_{14}Cu_{71}Ga_{15}$ (1 – $\tau_3$, 2 – $\tau_4$, 3 – Cu); (c) $U_{20}Cu_{30}Ga_{50}$ (1 – $\tau_5$, 2 – $\tau_2$); (d) $U_{22}Cu_{67}Ga_{11}$ (1 – $\tau_6$, 2 – $\tau_4$, 3 – α–U).

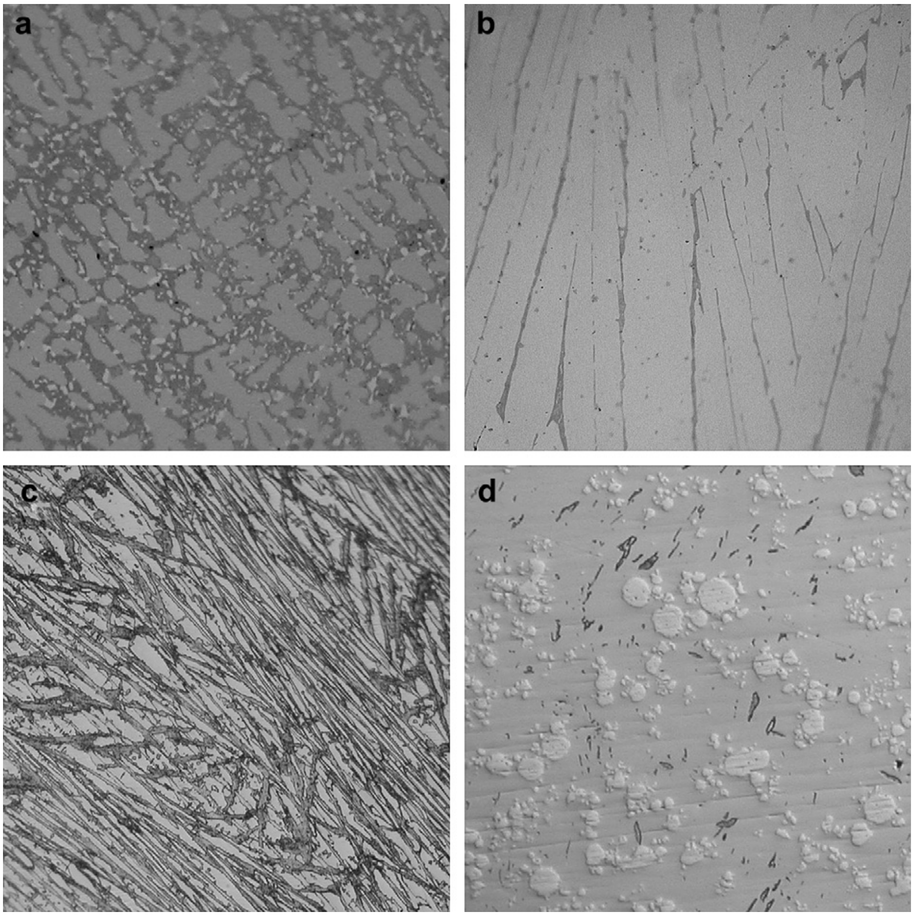

**Fig. 6.** Microphotographs of selected U–Cu–Ga alloys: (a) $U_{33}Cu_{33}Ga_{34}$ (×500), (b) $U_{20}Cu_{30}Ga_{50}$ (×200), (c) $U_{17}Cu_{76}Ga_7$ (×100) and (d) $U_{30}Cu_{63}Ga_7$ (×100).

**Table 3**
Ternary phases from the U–Cu–Ga system.

| Phase | Structure type | Space group | Lattice parameters | | | | x |
|---|---|---|---|---|---|---|---|
| | | | a | b | c | V | |
| $U_{2-\varepsilon}(Cu_{7+x}Ga_{10-x})_{1+\delta}$ ($\tau_1$) | Related to $Th_2Ni_{17}$ | *P*6$_3$/*mmc* | 8.8083(2) | – | 8.5835(2) | 576.74(2) | 0.5 |
| | | | 8.7975(3) | – | 8.5745(3) | 574.72(3) | 1 |
| $U_2Cu_{7+x}Ga_{10-x}$ ($\tau_2$) | $Th_2Zn_{17}$ | $R\overline{3}m$ | 8.7645(4) | – | 12.8134(7) | 852.41(7) | 2 |
| | | | 8.7276(2) | – | 12.7897(3) | 843.68(3) | 3 |
| | | | 8.7005(3) | – | 12.7600(5) | 836.50(6) | 4 |
| | | | 8.6871(5) | – | 12.6710(8) | 828.11(9) | 5 |
| $UCu_{5+x}Ga_{1-x}$ ($\tau_3$) | $CeCu_6$ | *Pnma* | 8.0253(6) | 4.9983(3) | 10.1752(7) | 408.16(5) | 0 |
| | | | 8.0187(7) | 4.9994(4) | 10.1417(9) | 406.57(6) | 0.3 |
| | | | 8.0172(3) | 5.0016(2) | 10.1018(4) | 405.07(3) | 0.5 |
| | | | 8.0172(8) | 5.0060(4) | 10.0746(9) | 404.34(6) | 0.7 |
| $UCu_{3+x}Ga_{2-x}$ ($\tau_4$) | $CaCu_5$ | *P*6/*mmm* | 5.1434(4) | – | 4.1300(3) | 94.62(1) | 0 |
| | | | 5.1162(2) | – | 4.1445(1) | 93.95(1) | 0.25 |
| | | | 5.0887(4) | – | 4.1511(3) | 93.09(1) | 0.5 |
| | | | 5.0787(3) | – | 4.1527(2) | 92.76(1) | 0.75 |
| $UCu_{1+x}Ga_{3-x}$ ($\tau_5$) | $BaAl_4$ | *I*4/*mmm* | 4.1512(2) | – | 10.0278(5) | 172.80(1) | 0.35 |
| | | | 4.1300(1) | – | 10.1430(4) | 173.01(1) | 0.5 |
| $U_{14}Cu_{44+x}Ga_{7-x}$ ($\tau_6$) | Related to $Gd_{14}Ag_{51}$ | *P*6/*m* | 11.6625(5) | – | 8.6248(4) | 1015.93(8) | 0.5 |
| | | | 11.6528(6) | – | 8.6212(5) | 1013.82(9) | 2.5 |

20 at.% Cu in the annealed alloys. The $Cu_{1-x}Ga_x$ solid solution (Cu-type) and intermediate phases, ht–$Cu_{0.78}Ga_{0.22}$ (Mg-type), ht–$Cu_9Ga_4$ ($Cu_9Al_4$-type) and rt–$Cu_9Ga_4$ (unknown type) are usually observed at the investigated temperature.

In the U–Cu–Ga system was confirmed the existence of the three early reported ternary phases and their homogeneity ranges at 600 °C: $U_2Cu_{7+x}Ga_{10-x}$ ($x \sim 2$–5) ($Th_2Zn_{17}$-type) ($\tau_2$), $UCu_{3+x}Ga_{2-x}$ ($x \sim 0$–0.8) ($CaCu_5$-type) ($\tau_4$) and $UCu_{1+x}Ga_{3-x}$ ($x \sim 0.35$–0.5) ($BaAl_4$-type) ($\tau_5$) (Table 3). The reported ternary gallides, $U_2CuGa_3$ ($Lu_2CoGa_3$-type) and UCuGa (LiGaGe-type), were not observed in the annealed U–Cu–Ga alloys. Herein, the $U_2CuGa_3$ (or $UCu_{0.5}Ga_{1.5} = U_{33}Cu_{17}Ga_{50}$) is a part of solid solution based on the binary $UGa_2$ compound. Annealed UCuGa ($=U_{33}Cu_{33}Ga_{34}$) alloy contains three phases ($\tau_4$, solid solution based on $UGa_2$ and $\alpha$-U) (Fig. 6a).

**Table 4**
Crystal data and structure refinement for $UCu_{5.5}Ga_{0.5}$.

| Empirical formula | $UCu_{5.5}Ga_{0.5}$ |
|---|---|
| Structure type | $CeCu_6$ |
| Crystal system | Orhtorhombic |
| Space group | *Pnma* |
| Pearson symbol | *oP*28 |
| Cell parameters | |
| *a* | 7.997(2) Å |
| *b* | 4.9871(12) Å |
| *c* | 10.115(4) Å |
| *V* | 403.4(2) Å$^3$ |
| Formula units per cell | 4 |
| Calculated density | 10.248 g/cm$^3$ |
| Crystal shape and colour | Irregular, silvery |
| Diffractometer | Enraf–Nonius Mach III |
| Wavelength | Mo-$K_\alpha$ ($\lambda = 0.71073$ Å) |
| Monochromator | Graphite |
| Temperature | 293(2) K |
| Absorption coefficient | 71.487 mm$^{-1}$ |
| F(000) | 1068 |
| $\theta$ range for data collection | 3.25°–41.04° |
| Scan type | $\omega$–2$\theta$ |
| Range in *hkl* | ±8, ±5, ±12 |
| Total no. reflections | 4182 |
| Independent reflection | 630 |
| Reflections with $I > 2\sigma(I)$ | 406 |
| Structure refinement | SHELXL-97 (Sheldrick-1997) |
| Refinement method | Full-matrix least-squares on $F^2$ |
| Data/restraints/parameters | 630/0/41 |
| Goodness-of-fit on *F* | 1.005 |
| Final *R* indices *R*1, *wR*2[a] | 0.0568, 0.0978 |
| Weighting scheme *a*, *b*[b] | 0.0104, 0 |
| Extinction coefficient | 0.0016(3) |
| Largest diff. peak/hole | 4.438/–3.849 e/Å$^3$ |

[a] $R1 = \sum(||F_o| - |F_c||)/\sum|F_o|, 5em wR2 = \{\sum w[(F_o^2 - F_c^2)^2]/\sum w[(F_o^2)^2]\}^{1/2}$;
[b] $w = 1/[\sigma^2(F_o^2) + (aP)^2 + bP]$, in which $P = [(F_o^2 + 2F_c^2)/3]$.

During the X-ray phase analysis of the as-cast and annealed alloys with composition closed to $U_{10}Cu_{40}Ga_{50}$ a new ternary gallide ($\tau_1$), with small homogeneity range, was found. Its crystal structure was solved from powder X-ray counter data of multiphase samples. Characteristic intensities of the peaks and indexing by a hexagonal unit cell with lattice parameters $a \sim 8.80$ Å and $c \sim 8.58$ Å indicated the $Th_2Ni_{17}$ structure type (space group *P*6$_3$/*mmc*). Rietveld method was applied for testing this model. However, the best results were obtained for the case of a defected model, where all atoms occupy the same sites as in the $Th_2Ni_{17}$ type with the exception of the 2*b* position, which is partially split into 4*e* site. Thus, the final composition of this phase was found to be $U_{2-\varepsilon}(Cu_{7+x}Ga_{10-x})_{1+\delta}$, with $\varepsilon \sim 0.5$, $\delta \sim 0.03$ and $x \sim 0.5$–1 and its lattice parameters can be found in Table 3. Nevertheless, synthesis and accurate characterization of single crystals are urgently needed.

In the as-prepared as well as in the annealed samples from the Cu-rich corner we found two new ternary phases and their crystal structures were studied on a basis of powder and single crystal X-ray diffraction data. Compositions and homogeneity ranges of these phases were established as $UCu_{5+x}Ga_{1-x}$ ($x \sim 0$–0.7) ($\tau_3$) and $U_{14}Cu_{44+x}Ga_{7-x}$ ($x \sim 0.5$–2.5) ($\tau_6$). Ternary gallides are derived from the $CeCu_6$ and $Gd_{14}Ag_{51}$ structure types. Calculated lattice parameters of selected alloys are shown in Table 3.

### 4.3. The $UCu_{5+x}Ga_{1-x}$ phase

The crystal structure of the $UCu_{5+x}Ga_{1-x}$ phase was fist refined by the Rietveld method on the basis of powder X-ray diffraction

**Table 5**
Atom coordinates and isotropic displacement parameters for $UCu_{5.5}Ga_{0.5}$.

| Atom | Site | x | y | z | $U_{eq}$(Å$^2$) | Occupation |
|---|---|---|---|---|---|---|
| U | 4*c* | 0.25799(15) | ¼ | 0.56181(9) | 0.0129(3) | 1 |
| M1 | 4*c* | 0.4049(5) | ¼ | 0.0165(3) | 0.0132(7) | 1 |
| M2 | 4*c* | 0.3186(4) | ¼ | 0.2547(3) | 0.0113(7) | 1 |
| M3 | 4*c* | 0.1432(4) | ¼ | 0.8570(3) | 0.0118(7) | 1 |
| M4 | 4*c* | 0.0632(5) | ¼ | 0.0926(3) | 0.0140(7) | 1 |
| M5 | 8*d* | 0.0659(3) | 0.5053(4) | 0.3082(2) | 0.0103(5) | 1 |

M = 0.92Cu + 0.08Ga.

**Table 6**
Anisotropic displacement parameters for $UCu_{5.5}Ga_{0.5}$.

| Atom | U11 | U22 | U33 | U23 | U13 | U12 |
|---|---|---|---|---|---|---|
| U | 0.0072(6) | 0.0165(5) | 0.0148(5) | 0 | −0.0005(4) | 0 |
| M1 | 0.011(2) | 0.0189(17) | 0.0091(14) | 0 | −0.0007(12) | 0 |
| M2 | 0.0035(17) | 0.0193(17) | 0.0112(14) | 0 | 0.0037(12) | 0 |
| M3 | 0.0066(19) | 0.0234(17) | 0.0054(13) | 0 | −0.0006(10) | 0 |
| M4 | 0.010(2) | 0.0207(18) | 0.0110(15) | 0 | −0.0002(13) | 0 |
| M5 | 0.0081(14) | 0.0146(12) | 0.0082(10) | −0.0011(7) | −0.0006(10) | −0.0003(8) |

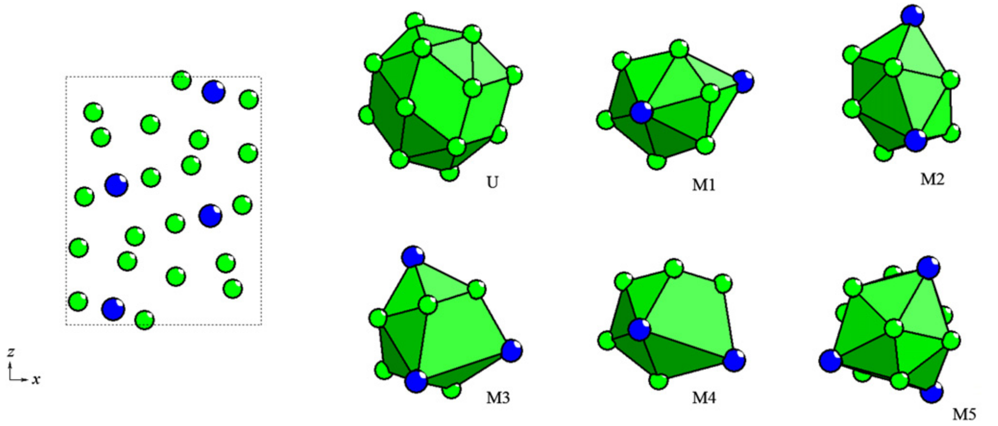

**Fig. 7.** Projection of the unit cell of the structure of $UCu_{5+x}Ga_{1-x}$ on the *xz* plane and coordination polyhedra of the atoms: U (big circles) and M (Cu and Ga) (small circles).

data. Starting positional parameters of the atoms were taken from the $CeCu_6$ structure type. Further studies were made on an irregular-shape single crystal extracted from the $U_{14.3}Cu_{78.7}Ga_7$ ($=UCu_{5.5}Ga_{0.5}$) alloy. Details of the data collection and structure refinement for $UCu_{5.5}Ga_{0.5}$ are given in Table 4. The refined values of the atomic coordinates and thermal displacement parameters are presented in Tables 5 and 6. All the crystallographic positions are fully occupied. Statistical mixtures of Cu and Ga were fixed during the refinement, as they are not distinguishable by X-ray diffraction.

The projection of the unit cell on the *xz* plane and coordination polyhedra of the atoms of the $UCu_{5+x}Ga_{1-x}$ structure are shown in Fig. 7. The neighbours of the U atoms form 19–vertex polyhedra, $[M1_3M2_3M3_4M4_3M5_6]$. The M1, M2, M3 and M5 atoms are

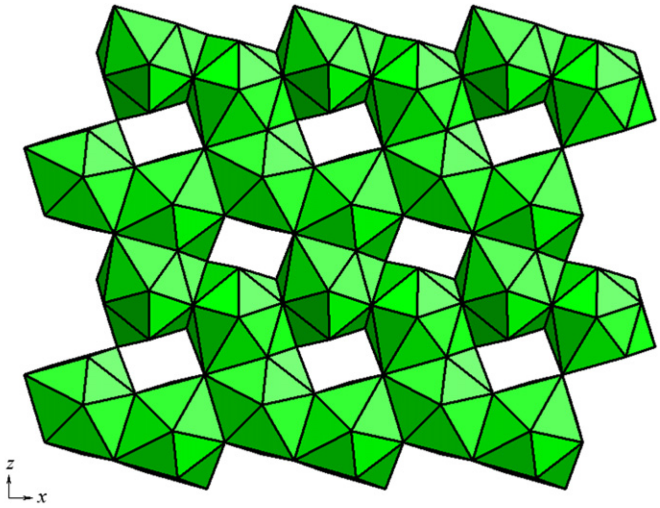

**Fig. 8.** Packing of icosahedrons in the structure of $UCu_{5+x}Ga_{1-x}$.

**Table 7**
Interatomic distances (*d*, Å) and coordination numbers (CN) for atoms in the structures of $UCu_{5.5}Ga_{0.5}$.

| Atoms | *d* | CN | Atoms | *d* | CN |
|---|---|---|---|---|---|
| U – | | 19 | M3 – | | 12 |
| – 2M1 | 2.850(2) | | – 1M4 | 2.467(4) | |
| – 2M4 | 2.891(2) | | – 1M1 | 2.642(5) | |
| – 1M4 | 2.898(4) | | – 2M5 | 2.660(4) | |
| – 1M1 | 2.933(4) | | – 2M5 | 2.673(4) | |
| – 2M5 | 3.112(2) | | – 2M2 | 2.717(2) | |
| – 1M3 | 3.124(3) | | – 1U | 3.124(3) | |
| – 1M2 | 3.144(3) | | – 1U | 3.188(3) | |
| – 2M5 | 3.151(3) | | – 2U | 3.337(2) | |
| – 1M3 | 3.188(3) | | | | |
| – 2M2 | 3.225(2) | | M4 – | | 9 |
| – 2M5 | 3.250(2) | | – 1M3 | 2.467(4) | |
| – 2M3 | 3.337(2) | | – 1M2 | 2.492(5) | |
| | | | – 2M5 | 2.525(3) | |
| M1 – | | 12 | – 1M2 | 2.619(5) | |
| – 2M5 | 2.446(3) | | – 1M1 | 2.839(6) | |
| – 1M2 | 2.506(4) | | – 2U | 2.891(2) | |
| – 2M5 | 2.534(4) | | – 1U | 2.898(4) | |
| – 1M3 | 2.642(5) | | | | |
| – 1M4 | 2.839(6) | | M5 – | | 12 |
| – 2U | 2.850(2) | | – 1M2 | 2.437(4) | |
| – 1U | 2.933(4) | | – 1M5 | 2.441(3) | |
| – 2M1 | 2.940(3) | | – 1M1 | 2.446(3) | |
| | | | – 1M2 | 2.449(4) | |
| M2 – | | 12 | – 1M4 | 2.525(3) | |
| – 2M5 | 2.437(4) | | – 1M1 | 2.534(4) | |
| – 2M5 | 2.449(4) | | – 1M5 | 2.546(3) | |
| – 1M4 | 2.492(5) | | – 1M3 | 2.660(4) | |
| – 1M1 | 2.506(4) | | – 1M3 | 2.673(4) | |
| – 1M4 | 2.619(5) | | – 1U | 3.112(2) | |
| – 2M3 | 2.717(2) | | – 1U | 3.151(3) | |
| – 1U | 3.144(3) | | – 1U | 3.250(2) | |
| – 2U | 3.225(2) | | | | |

**Table 8**
Crystal data and structure refinement for $U_{14}Cu_{46}Ga_5$.

| Empirical formula | $U_{14}Cu_{46}Ga_5$ |
|---|---|
| Structure type | Related to $Gd_{14}Ag_{51}$ |
| Crystal system | Hexagonal |
| Space group | *P*6/*m* |
| Pearson symbol | *hP*68 |
| Cell parameters | |
| *a* | 11.650(2) Å |
| *c* | 8.6020(15) Å |
| *V* | 1011.1(3) $Å^3$ |
| Formula units per cell | 1 |
| Calculated density | 10.795 $g/cm^3$ |
| Crystal shape and colour | Irregular, silvery |
| Diffractometer | Enraf–Nonius Mach III |
| Wavelength | Mo-$K_\alpha$ ($\lambda = 0.71073$ Å) |
| Monochromator | Graphite |
| Temperature | 293(2) K |
| Absorption coefficient | 81.931 $mm^{-1}$ |
| F(000) | 2767 |
| $\theta$ range for data collection | 2.02°–44.88° |
| Scan type | $\omega$–$2\theta$ |
| Range in *hkl* | ±13, ±13, ±10 |
| Total no. reflections | 14,390 |
| Independent reflection | 1839 |
| Reflections with $I > 2\sigma(I)$ | 659 |
| Structure refinement | SHELXL-97 (Sheldrick-1997) |
| Refinement method | Full-matrix least-squares on $F^2$ |
| Data/restraints/parameters | 1839/0/64 |
| Goodness-of-fit on *F* | 1.000 |
| Final *R* indices *R*1, *wR*2[a] | 0.0647, 0.0884 |
| Weighting scheme *a*, *b*[b] | 0.0277, 0 |
| Extinction coefficient | 0.00035(6) |
| Largest diff. peak/hole | 3.717/–5.621 e/$Å^3$ |

[a] $R1 = \sum(||F_o| - |F_c||)/\sum|F_o|, 5emwR2 = \{\sum w[(F_o^2 - F_c^2)^2]/\sum w[(F_o^2)^2]\}^{1/2}$;

[b] $w = 1/[\sigma^2(F_o^2) + (aP)^2 + bP]$, in which $P = [(F_o^2 + 2F_c^2)/3]$.

**Table 9**
Atom coordinates and isotropic displacement parameters for $U_{14}Cu_{46}Ga_5$.

| Atom | Site | *x* | *y* | *z* | $U_{eq/iso}$($Å^2$) | Occupation |
|---|---|---|---|---|---|---|
| U1 | 2*e* | 0 | 0 | 0.3086(3) | 0.0050(5) | 1 |
| U2A | 6*j* | 0.1114(6) | 0.3654(12) | 0 | 0.0065(14) | 0.45(3) |
| U2B | 6*j* | 0.1286(5) | 0.4071(9) | 0 | 0.0067(11) | 0.57(3) |
| U3 | 6*k* | 0.47068(16) | 0.13838(16) | ½ | 0.0061(4) | 1 |
| M1 | 2*c* | 1/3 | 2/3 | 0 | 0.028(3) | 1 |
| (M1)[a] | 6*j* | 0.330(4) | 0.688(3) | 0 | 0.004(4) | 0.336(13) |
| M2 | 4*h* | 1/3 | 2/3 | 0.2761(6) | 0.0045(12) | 1 |
| M3 | 6*j* | 0.0405(11) | 0.1390(10) | 0 | 0.006(3) | 0.494(19) |
| M4 | 6*k* | 0.0630(5) | 0.2412(5) | ½ | 0.0074(11) | 1 |
| M5 | 12*l* | 0.4938(4) | 0.1081(4) | 0.1538(4) | 0.0085(8) | 1 |
| M6 | 12*l* | 0.2687(3) | 0.0695(4) | 0.2452(4) | 0.0105(8) | 1 |
| M7 | 12*l* | 0.1085(4) | 0.4355(4) | 0.3257(4) | 0.0091(8) | 1 |

M = 0.90Cu + 0.10Ga.

[a] An alternatively atomic position of M1 atoms in the disordered model.

located inside deformed icosahedra (coordination number 12), $[U_3M1_2M2_1M3_1M4_1M5_4]$, $[U_3M1_1M3_2M4_2M5_4]$, $[U_4M1_1M2_2M4_1M5_4]$ and $[U_3M1_2M2_2M3_2M4_1M5_2]$, respectively. The 9-vertex polyhedra, $[U_3M1_1M2_2M3_1M5_2]$, are coordination spheres of the M4 atoms. The $UCu_{5+x}Ga_{1-x}$ structure can be composed by stacking of the icosahedra around the M5 atoms. These icosahedra are connected along the *y* axis by the vertexes with shared M5 atoms, and along the direction parallel to the *xz* plane by triangle faces (Fig. 8). From this point of view the structure can be seen as a layered one, where two types of layers (*A* and *B*) form a sequence *ABAB′* along [010] direction. *A* layer (a distorted $6^3$ net) is composed by M atoms, while *B* layer (3535, $3^25^2$, $3^25^3$ and $3^45$ net) and its 180° rotated analogue, *B′*, are formed by U and M atoms.

Interatomic distances (*d*) in the $UCu_{5+x}Ga_{1-x}$ structure are presented in Table 7. These distances are in general close to the sum of the atomic radii of the respective atoms [33]. Significant shorter distances (with *d* less then $2r_{atomic}$) can be found for M–M atoms, which are indication of strong interactions between these atoms. The minimum $d_{M-M}$ was found with 2.437 Å (value of reducing $\Delta \sim 5\%$).

### 4.4. The $U_{14}Cu_{44+x}Ga_{7-x}$ phase

The primary analysis of powder X-ray diffraction data of the as-cast and annealed $U_{14}Cu_{44+x}Ga_{7-x}$ samples pointed out to the $Gd_{14}Ag_{51}$ structure type for the above sited phase. Investigation of an irregular-shape single crystal, isolated from crushed $U_{21.5}Cu_{70.8}Ga_{7.7}$ (=$U_{14}Cu_{46}Ga_5$) sample, was conducted considering this model. Crystal data and structure refinement results are displayed in Table 8. Final atom coordinates, site occupancies and displaced parameters for the $U_{14}Cu_{46}Ga_5$ structure are listed in Tables 9 and 10. The present results indicated a $Gd_{14}Ag_{51}$-based structure type for $U_{14}Cu_{46}Ga_5$, with the uranium atoms in the layer at $z = 0$ splitted into two half-occupied 6*j* positions (U2A and U2B sites). Large displacement parameters of M1 atoms are observed in this structure, which can indicate possible atom disorder of the 2*c* position. Similar disorder of atoms can also be found in the structure of the $Ce_{14}Cu_{51}$ type (2*c* is splitted into 6*j*). However, parallel structure refinement using this last model does not give better results.

The unit cell and coordination polyhedra of the atoms are presented in Fig. 9. The number of the neighbours for uranium atoms varies from 13 to 16. Coordination spheres can be presented as $[U1_1M3_3M4_6M6_6]$ (CN = 16), $[M1_1M5_6M6_4M7_2]$ (CN = 13), $[M1_1M3_1M5_6M6_4M7_2]$ (CN = 14), $[M2_2M4_2M5_2M6_2M7_6]$ (CN = 14) for U1, U2A, U2B and U3 atoms, and they have similar details with 14-vertex Frank–Kasper polyhedron. The M1 atoms are located inside full-capped trigonal prisms $[U2B_3M2_2M5_6]$ (CN = 11). Four-capped deformed trigonal prisms, $[U3_3M1_1M5_3M7_3]$ (CN = 10), are polyhedra for the M2 atoms. Polyhedra (deformed full capped trigonal prisms) of the M3 atoms consist of eleven neighbouring atoms $[U1_2U2A_2U2B_1M3_2M6_4]$. The M4 and M6 atoms are coordinated by distorted icosahedra (CN = 12), $[U1_2U3_2M4_2M6_4M7_2]$ and $[U1_1U2A_2U3_1M3_1M4_2M5_1M6_2M7_2]$, respectively. 11- and 10-vertex polyhedra (somewhat like a defected icosahedra), $[U2B_3U3_1M1_1M2_1M5_2M6_1M7_2]$ and $[U2B_1U3_3M2_1M4_1M5_2M6_2]$, are the coordination spheres for M5 and M7 atoms, respectively.

**Table 10**
Anisotropic displacement parameters for $U_{14}Cu_{46}Ga_5$.

| Atom | U11 | U22 | U33 | U23 | U13 | U12 |
|---|---|---|---|---|---|---|
| U1 | 0.0039(8) | 0.0039(8) | 0.0074(11) | 0 | 0 | 0.0019(4) |
| U3 | 0.0040(8) | 0.0070(8) | 0.0081(6) | 0 | 0 | 0.0032(7) |
| M1 | 0.040(5) | 0.040(5) | 0.005(5) | 0 | 0 | 0.020(3) |
| M2 | 0.0019(18) | 0.0019(18) | 0.010(3) | 0 | 0 | 0.0009(9) |
| M3 | 0.007(6) | 0.002(6) | 0.005(5) | 0 | 0 | –0.001(4) |
| M4 | 0.005(3) | 0.004(3) | 0.009(2) | 0 | 0 | –0.001(2) |
| M5 | 0.007(2) | 0.008(2) | 0.0090(15) | 0.0013(13) | –0.0007(14) | 0.0025(16) |
| M6 | 0.0037(18) | 0.022(2) | 0.0058(14) | 0.0005(16) | 0.0000(13) | 0.0064(17) |
| M7 | 0.011(2) | 0.0056(19) | 0.0090(16) | 0.0024(12) | 0.0002(13) | 0.0029(17) |

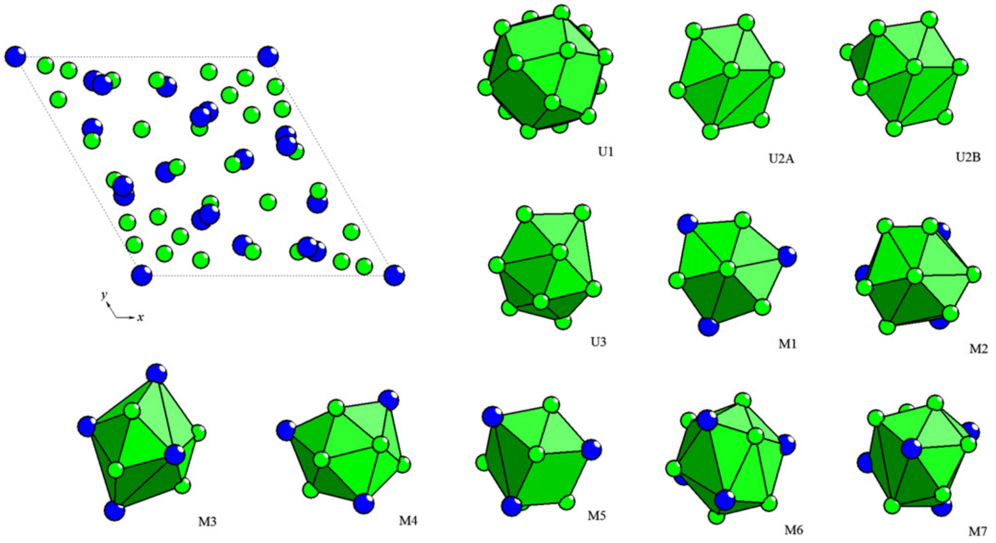

**Fig. 9.** Projection of the unit cell of the structure of $U_{14}Cu_{44+x}Ga_{7-x}$ on the *xy* plane and coordination polyhedra of the atoms: U (big circles) and M (Cu and Ga) (small circles).

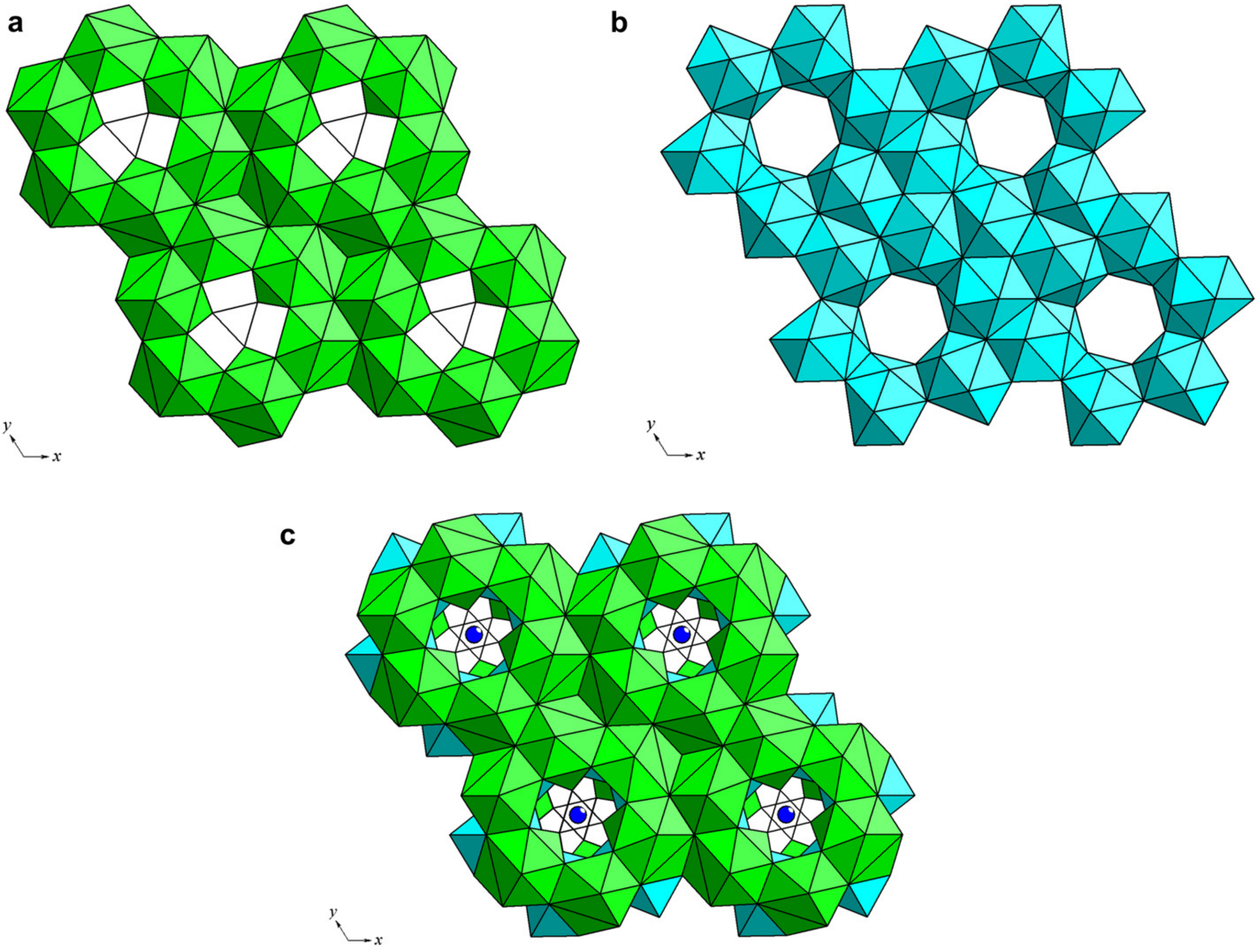

**Fig. 10.** An aggregation of the hexagonal like wheel composed by the coordination polyhedra of the U2A, U2B (a) and U3 (b) atoms, and their packing (c) in the structure of $U_{14}Cu_{44+x}Ga_{7-x}$.

**Table 11**
Interatomic distances and coordination polyhedra of the atoms in the structures of $U_{14}Cu_{46}Ga_5$.

| Atoms | *d* | CN | Atoms | *d* | CN |
|---|---|---|---|---|---|
| U1 – | | 16 | M4 – | | 12 |
| – 6M6 | 2.867(3) | | – 2M4 | 2.524(5) | |
| – 6M4 | 3.014(4) | | – 2M7 | 2.540(6) | |
| – 3M3 | 3.021(5) | | – 2M6 | 2.583(5) | |
| – 1U1 | 3.293(4) | | – 2M6 | 2.630(4) | |
| | | | – 1U3 | 2.933(4) | |
| U2A – | | 13 | – 2U1 | 3.014(5) | |
| – 2M6 | 2.814(10) | | – 1U3 | 3.020(7) | |
| – 2M7 | 2.923(6) | | | | |
| – 2M6 | 2.926(6) | | M5 – | | 11 |
| – 2M5 | 2.992(10) | | – 1M6 | 2.553(6) | |
| – 2M5 | 3.069(6) | | – 1M7 | 2.556(5) | |
| – 1M1 | 3.151(10) | | – 1M5 | 2.594(7) | |
| – 2M5 | 3.205(13) | | – 1M2 | 2.601(4) | |
| | | | – 1M5 | 2.646(5) | |
| U2B – | | 14 | – 1M1 | 2.722(3) | |
| – 1M3 | 2.757(15) | | – 1M7 | 2.725(5) | |
| – 1M1 | 2.760(7) | | – 1U2B | 2.865(7) | |
| – 2M7 | 2.844(4) | | – 1U2B | 2.952(10) | |
| – 2M5 | 2.865(10) | | – 1U2B | 2.955(5) | |
| – 2M5 | 2.952(6) | | – 1U3 | 3.027(4) | |
| – 2M5 | 2.954(8) | | | | |
| – 2M6 | 3.009(8) | | M6 – | | 12 |
| – 2M6 | 3.170(5) | | – 1M5 | 2.553(6) | |
| | | | – 1M7 | 2.579(7) | |
| U3 – | | 14 | – 1M4 | 2.583(4) | |
| – 2M7 | 2.854(4) | | – 1M4 | 2.630(5) | |
| – 2M7 | 2.917(4) | | – 1M3 | 2.712(8) | |
| – 1M4 | 2.933(6) | | – 1M7 | 2.725(4) | |
| – 2M7 | 2.957(4) | | – 2M6 | 2.814(4) | |
| – 2M2 | 2.982(3) | | – 1U2A | 2.814(5) | |
| – 2M6 | 3.016(4) | | – 1U1 | 2.867(4) | |
| – 1M4 | 3.020(2) | | – 1U2A | 2.926(7) | |
| – 2M5 | 3.027(4) | | – 1U3 | 3.016(4) | |
| M1 – | | 11 | M7 – | | 10 |
| – 2M2 | 2.375(5) | | – 1M4 | 2.540(6) | |
| – 6M5 | 2.722(3) | | – 1M5 | 2.556(5) | |
| – 3U2B | 2.760(7) | | – 1M6 | 2.579(4) | |
| | | | – 1M2 | 2.691(3) | |
| M2 – | | 10 | – 1M5 | 2.725(6) | |
| – 1M1 | 2.375(5) | | – 1M6 | 2.725(7) | |
| – 3M5 | 2.601(4) | | – 1U2B | 2.844(4) | |
| – 3M7 | 2.691(3) | | – 1U3 | 2.854(5) | |
| – 3U3 | 2.982(3) | | – 1U3 | 2.917(4) | |
| | | | – 1U3 | 2.957(5) | |
| M3 – | | 11 | | | |
| – 2M3 | 2.499(9) | | | | |
| – 2M6 | 2.712(6) | | | | |
| – 2M6 | 2.735(10) | | | | |
| – 1U2B | 2.757(15) | | | | |
| – 2U1 | 3.021(6) | | | | |
| – 1U2A | 3.282(16) | | | | |
| – 1U2A | 3.324(18) | | | | |

The structure of $U_{14}Cu_{44+x}Ga_{7-x}$ can be seen as a packing of two different types of layers (slabs) along the *z* direction. These layers are the aggregation of the six-membered wheel, which are composed by the coordination polyhedra of the U2A, U2B and U3 atoms (Fig. 10a and b). The hexagonal cavities, which are located in the centres of these wheels, are filled by the U1 atoms (Fig. 10c).

Interatomic distances in the $U_{14}Cu_{44+x}Ga_{7-x}$ are close to the sum of the atomic radii in the pure metals [33] and are listed in Table 11. The shortest bonds for U–M atoms are equal to 2.757 Å ($\Delta \sim 2\%$) and those for the M–M atoms amount to 2.375 Å ($\Delta \sim 7\%$).

## 5. Conclusion

Isothermal sections of the phase diagram of the U–Cu–Al and U–Cu–Ga systems have been constructed at 600 °C by means of X-ray diffraction, optical microscopy and scanning electronic microscopy. The interaction of the components in these systems leads to the formation of twelve ternary phases (five of them reported here for the first time): $UCu_{4+x}Al_{8-x}$ ($x \sim 0$–$2$), $UCu_{6+x}Al_{5-x}$ ($x \sim 0$–$0.2$), $UCu_{6+x}Al_{5-x}$ ($x \sim 0.38$–$0.68$), $U_2Cu_{7+x}Al_{10-x}$ ($x \sim 0.6$–$5$), $UCu_{5+x}Al_{1-x}$ ($x \sim 0$–$0.18$), $UCu_{3+x}Al_{2-x}$ ($x \sim 0$–$0.5$) and $U_{2-\varepsilon}(Cu_{7+x}Ga_{10-x})_{1+\delta}$ ($\varepsilon \sim 0.5$, $\delta \sim 0.03$, $x \sim 0.5$–$1$), $U_2Cu_{7+x}Ga_{10-x}$ ($x \sim 2$–$5$), $UCu_{5+x}Ga_{1-x}$ ($x \sim 0$–$0.7$), $UCu_{3+x}Ga_{2-x}$ ($x \sim 0$–$0.8$), $UCu_{1+x}Ga_{3-x}$ ($x \sim 0.35$–$0.5$), $U_{14}Cu_{44+x}Ga_{7-x}$ ($x \sim 0.5$–$2.5$), respectively. All these compounds are formed in the region with less than 33.3 at.% U. Binary $UAl_2$ and $UGa_2$ compounds form solid solutions by the Cu/Al or Cu/Ga substitutions. The available data on the U–Cu–Al and U–Cu–Ga systems point to the possibility of identification of new ternary phases in the yet unexplored systems with actinides.

## Acknowledgements

This work was partially supported by FCT, Portugal, under the contract No. PTDC/CTM/102766/2008. The FCT Grant No. SFRH/BPD/34840/2007 for the research work of Y.V. at ITN, Sacavém, Portugal is highly appreciated. The authors would like to express their gratitude to Dr. Nuno Leal from Universidade Nova de Lisboa (Caparica, Portugal) for the help during SEM/EDS studies.

## Appendix A. Supplementary data

Supplementary data related to this article can be found at http://dx.doi.org/10.1016/j.intermet.2012.09.024.

## References

[1] Sechovsky V, Havela L. Intermetallic compounds of actinides. In: Wohlfarth EP, Buschow KHJ, editors. Ferromagnetic materials – a handbook on the properties of magnetically ordered substances, vol. 4. North-Holland, Amsterdam: Elsevier Science Publishers B.V; 1988. p. 309–491.
[2] Hlukhyy VV. Interaction of the components in the U–{Co, Ni, Cu}–In and related systems. Thesis. Ukraine, Lviv; 2003.
[3] Hluhyy V, Zaremba V, Nychyporuk G. Investigation of interaction of compounds in the ternary system U–Ni–In at 870 K. Visnyk Lviv Univ Ser Khim 2007;48(1):161–5.
[4] Zelinskiy AV. Interaction of components in the U–{Fe, Co, Ni}–Ga ternary systems. Thesis. Ukraine, Lviv; 2010.
[5] SpringerMaterials, the Landolt-Börnstein database, http://www.springermaterials.com; 2012.
[6] Gordon P, Kaufmann AR. Uranium–aluminum and uranium–iron. Trans Am Inst Min Metall Pet Eng 1950;188:182–94.
[7] Buschow KHJ. Phase relationships and magnetic properties of uranium–gallium compounds. J Less-Common Met 1973;31:165–8.
[8] Wilhelm HA, Carlson ON. The uranium–manganese and uranium–copper alloy systems. Trans Am Soc Met 1950;42:1311–25.
[9] Murray JL. The aluminium–copper system. Int Met Rev 1985;30:211–33.
[10] Ponweiser N, Lengauer CL, Richter KW. Re-investigation of phase equilibria in the system Al–Cu and structural analysis of the high-temperature phase $\eta_1$–$Al_{1-\delta}Cu$. Intermetallics 2011;19:1737–46.
[11] Betterton JO, Hume Rothery W. The equilibrium diagram of the system copper–gallium in the region 30–100 at.% gallium. J Inst Met 1951/52;80: 459–68.
[12] Subramanian PR, Laughlin DE. In: Massalski TB, editor. Cu–Ga (copper–gallium), binary alloy phase diagrams. 2nd ed., vol. 2; 1990. p. 1410–2.
[13] Sechovsky V, Havela L. Magnetism of ternary intermetallic compounds of uranium. In: Buschow KHJ, editor. Handbook of magnetic materials, vol. 11. North-Holland, Amsterdam: Elsevier Science B.V; 1998. p. 1–289.
[14] Blažina Ž, Ban Z. The crystal structures of $U_2Cu_3Al$ and $UCuAl_2$, and their relationship with some other phases in the system U–Cu–Al. Z Naturforsch 1980;35b:1162–5.
[15] Blažina Ž, Ban Z. The crystal structures of $U_2Cu_9Al$ and $UCu_{3.5}Al_{1.5}$. Z Naturforsch 1973;28b:561–4.
[16] Nakotte H, Brück E, Brabers JHVJ, Prokeš K, de Boer FR, Sechovsky V, et al. Magnetic properties of single-crystalline $UCu_3Al_2$. IEEE Trans Magn 1994;30: 1217–9.
[17] Troc R, Tran VH, Wolcyrz M, Andre G, Bouree F. Crystal and magnetic structure of a novel compound $UCu_5Al$. Structural stability with Th-substitution. J Magn Magn Mat 1998;190:251–6.

[18] Cordier G, Czech E, Schäfer H, Woll P. Structural characterization of new ternary compounds of uranium and cerium. J Less-Common Met 1985;110:327–30.

[19] Troć R, Andraka B, Kuznietz M, Tran VH, Gurevich AM, Wolcyrz M, et al. Heavy-fermion behaviour in the $Th_2Zn_{17}$-type pseudobinary systems $U_2(Cu, M)_{17}$ (M = Al or Ga). Physica B 1997;230–232:65–7.

[20] Geibel C, Ahlheim U, Giorgi AL, Sparn G, Spille H, Steglich F, et al. Formation of heavy fermion phase in $UCu_{4+x}Al_{8-x}$ by variation of stoichiometry. Physica B 1990;163:194–6.

[21] Stępień–Damm J, Tran VH, Shlyk L, Troć R. Crystal structure of $U_2Ga_{5-x}Ga_{12}$. J Alloys Compd 1994;205:291–3.

[22] Zolnierek Z, Szulc E. Magnetic and electrical properties of the tetragonal $U(Cu, Ni)_{2-x}Ga_{2+x}$ phases. J Alloys Compd 1992;187:255–62.

[23] Takabatake T, Maeda Y, Fujii H, Ikeda S, Nishigori S, Fujita T, et al. Structural and physical properties of new U–T–Ga compounds (T = Ni, Cu and Pd). Physica B Condens Mat 1993;186–188:734–7.

[24] Kurisu M, Takahashi T, Maeda Y, Iwasaki H, Takabatake T, Fujii H. Effect of pressure on the magnetic superzone gap in antiferromagnetic uranium compounds $UCu_2Sn$ and $UCu_3Ga_2$. Physica B Condens Mat 1993;186–188:766–8.

[25] Tran VH, Troć R, Badurski D. Magnetic and transport properties of UCuGa, $U_2CuGa_3$ and UAuGa. J Alloys Compd 1993;199:193–6.

[26] Tran VH, Daczorowski D, Roisnel T, Troć R, Noël H, Bourée F, et al. Magnetic properties of UCuGa and $U_2CuGa_3$ by AC–magnetic susceptibility and neutron diffraction. Physica B 1995;205:24–30.

[27] Gandra FG, Rojas DP, Shlyk L, Cardoso LP, Medina AN. Magnetic phase diagram of $U(Ga_{1-x}Cu_x)_2$. J Magn Magn Mater 2001;226–230:1312–4.

[28] Nolze G, Kraus W. Powder cell for Windows (version 2.3). Berlin: Federal Institute for Materials Research and Testing; 1999.

[29] Schwarzenbach D. Program LATCON. Switzerland: University of Lausanne; 1975.

[30] Rodriguez–Carvajal J, Roisnel T. FullProf.98 and WinPLOTR: new Windows 95/NT applications for diffraction commission for powder diffraction. Int Union Crystallogr Newsl May–August, Summer, 1998;(20).

[31] Sheldrick GM. SHELX-97, a program system for the solution and refinement of crystal structures. Germany: Universität Göttingen; 1997.

[32] Nakote H, Buschow KHJ, Klaasse JCP, Prokeš K, de Boer FR, Andreev AV, et al. Possible heavy-fermion behaviour of new $U(Cu, Al)_5$ compounds. J Magn Magn Mat 1995;140–144:1261–2.

[33] Bokiy GB. Crystal chemistry. 3rd ed. Moscow: Nauka; 1971 [in Russian].